SAND79-8266

Unlimited Release

Comparison Between Results of the HELIOS and MIRVAL Computer Codes Applied to Central Receiver Solar-Energy Collection

C. N. Vittitoe, F. Biggs, P. L. Leary

Prepared by Sandia Laboratories, Albuquerque, New Mexico 87115 and Livermore, California 94550 for the United States Department of Energy under Contract DE-AC04-76DP00789.

Printed January 1980

Sandia Laboratories

energy report

SF 2900-QQB(3-74)

Issued by Sandia Laboratories, operated for the United States Department of Energy by Sandia Corporation.

NOTICE

Printed in the United States of America
Available from
National Technical Information Service
U. S. Department of Commerce
5285 Port Royal Road
Springfield, VA 22161
Price: Printed Copy $4.50; Microfiche $3.00

SAND79-8266
Unlimited Release
Printed January 1980

COMPARISON BETWEEN RESULTS OF THE HELIOS AND MIRVAL COMPUTER CODES APPLIED TO CENTRAL RECEIVER SOLAR-ENERGY COLLECTION*

Charles N. Vittitoe
Frank Biggs
Theoretical Division
Sandia Laboratories, Albuquerque

Patricia L. Leary
Applied Mathematics Division
Sandia Laboratories, Livermore

ABSTRACT

The Sandia computer codes HELIOS and MIRVAL were developed to predict the optical performance of reflecting solar concentrators and to model power collection by central-receiver solar-energy power plants. HELIOS is an analytic code, whereas MIRVAL uses Monte Carlo ray-tracing techniques. They have been used both internally and externally in many studies including evaluation of heliostat-receiver design, parameter studies and safety analyses. The objective of this study was to verify that HELIOS and MIRVAL give the same performance predictions. The sample problem for comparison consists of a rectangular target and alt-azimuth heliostats deployed in a north field. The results indicate that HELIOS and MIRVAL closely agree on predictions of field performance and of power density on the target plane.

---

*This work supported by the U. S. Department of Energy.

CONTENTS

COMPARISON BETWEEN RESULTS OF THE HELIOS AND MIRVAL COMPUTER CODES APPLIED TO CENTRAL RECEIVER SOLAR-ENERGY COLLECTION

Introduction

Harnessing solar power economically is a tremendous undertaking, with many possibilities for expensive waste. Computer codes have been developed to simulate various methods of collecting solar energy in order to avoid mistakes new technology can bring. The low cost of computer use compared with that of hardware development allows for many parametric studies prior to hardware decisions.

Because of the expense associated with high-accuracy hardware, solar-energy development seeks a trade-off between accuracy and cost. One of the largest expenses is in the heliostats (mirror array). In the optimum design, the cost (and therefore accuracy) is minimized subject to the constraint that we receive the desired power and the desired distribution of power on the receiver. Since computer models aid in making decisions involving large hardware expenditures, it is important that the models be verified comparatively and experimentally.

MIRVAL and HELIOS are two computer codes that are used to assess the overall optical performance of systems proposed for central receiver solar-energy collection. Documentation of the theory and use of these codes appears elsewhere.[1-3] Briefly, the inputs are the geometry of the heliostat field, tower, and receiver, along with miscellaneous physical data such as mirror reflectivity, insolation tables, etc., and the outputs are the thermal power through the receiver and the thermal power density on the plane of the receiver opening. Phenomena whose effects are simulated are shadowing, blocking, mirror tracking, random errors in tracking and in the conformation of the reflective surface, optical shape of the reflective surface, insolation, angular distribution of incoming sun rays to account for limb darkening and scattering, attenuation of light between the mirrors and the receiver, reflectivity of the mirror surface, and mirror-aiming strategy.

The methodologies of HELIOS and MIRVAL are quite different. MIRVAL is a Monte Carlo code. Rays of light are selected from the vicinity of the sun and are traced until they either enter the receiver or are lost in a prior absorption process or are deflected enough to miss the receiver. HELIOS, on the other hand, is an analytic code. The angular distribution of sunrays for the radiation incident on a concentrator is modified by convolution, using the fast Fourier transform, to incorporate the effects of other nondeterministic factors such as sun-tracking errors, surface slope errors, and reflectance properties.

MIRVAL has been used to compare sets of heliostat-field, tower-receiver, heliostat, and facet designs that have been proposed for the 10-MW electical power tower now planned for Barstow, California. HELIOS has been used in the evaluation of individual heliostats at the Central Receiver Test Facility (CRTF) now in operation at Sandia Laboratories, Albuquerque, New Mexico. We tested several designs which had been proposed for the Barstow plant. MIRVAL and HELIOS have also been used in many other types of studies: safety analysis, parameter studies, power-tower-performance calculations, and comparison with experimental data.

Several previous checks of HELIOS were described in Chapter 9 of Reference 2. All of the quantitative comparisons with experiment were either for one heliostat or for one facet. Such comparisons give no validation to code features such as shadowing and blocking. Other work[4] examined consistency between prediction and experiment for a small field of 23 heliostats. As indicated elsewhere[2] detailed flux-density measurements are planned for the CRTF using large heliostat arrays and concurrent sunshape data. These data in turn will be used as experimental data for similar comparisons. This report examines the consistency of the two computer codes when applied to larger heliostat fields. We detail the basic input used to compare the codes, including the basic power-tower optical design. The code outputs described indicate that MIRVAL and HELIOS results are consistent.

Because often-used computer codes associated with a rapidly evolving technology are revised frequently to meet new demands, comparison is constrained to the versions of MIRVAL and HELIOS in use during July 1979. It is expected, however, that future versions of the codes will not alter the basic results or conclusions presented here.

Code Input

As a result of interaction with a group from the Empresa Nacional de Ingenieria Y Technologia (INITEC) in Madrid, both MIRVAL and HELIOS were used to aid in the design of the 1-MW_e CESA-1 (Central Energia Solar Almeria) solar-central receiver plant being built in Almeria, Spain. The preliminary design of the CESA-1 system (but with a spherical facet-surface shape) provided the details for the code comparison between HELIOS and MIRVAL.

The mirror array consists of 282 heliostats deployed in a north field, as shown in Figure 1. This figure was produced by HELIOS, as were all other computer graphics in this report. The coordinates of the heliostats are listed in the Appendix.

HELIOSTAT LAYOUT IN EAST - NORTH PLANE

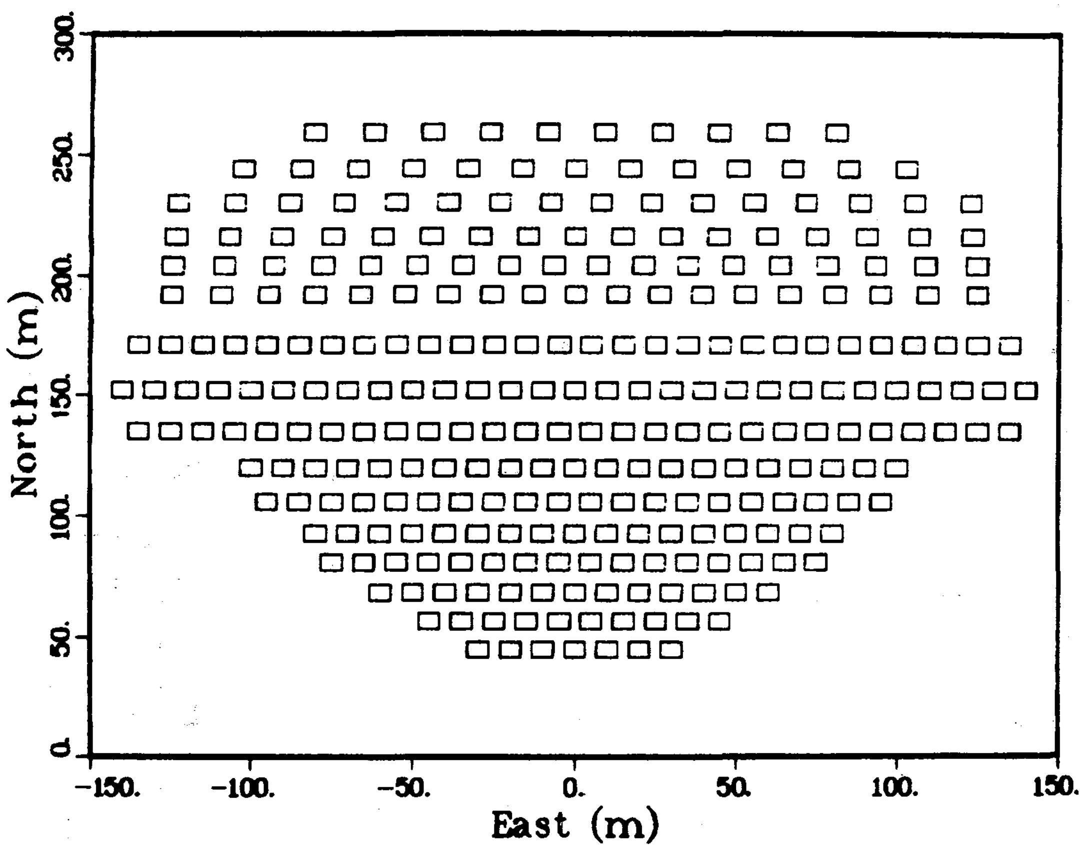

Figure 1. Preliminary Heliostat Layout in East-North Plane for the CESA-1 Solar Central-Receiver Project

All are aimed at the center of the target. Each heliostat consists of 10 panels arranged in a 2 x 5 pattern (Figure 2). Individual facets are canted to give optimum energy collection at noon on solar equinox. The facet surfaces are spherical with a reflectivity of 0.85. The focal length of each facet is determined from the projection P of the heliostat to tower-center distance onto a horizontal plane. The f values are listed in Table I.

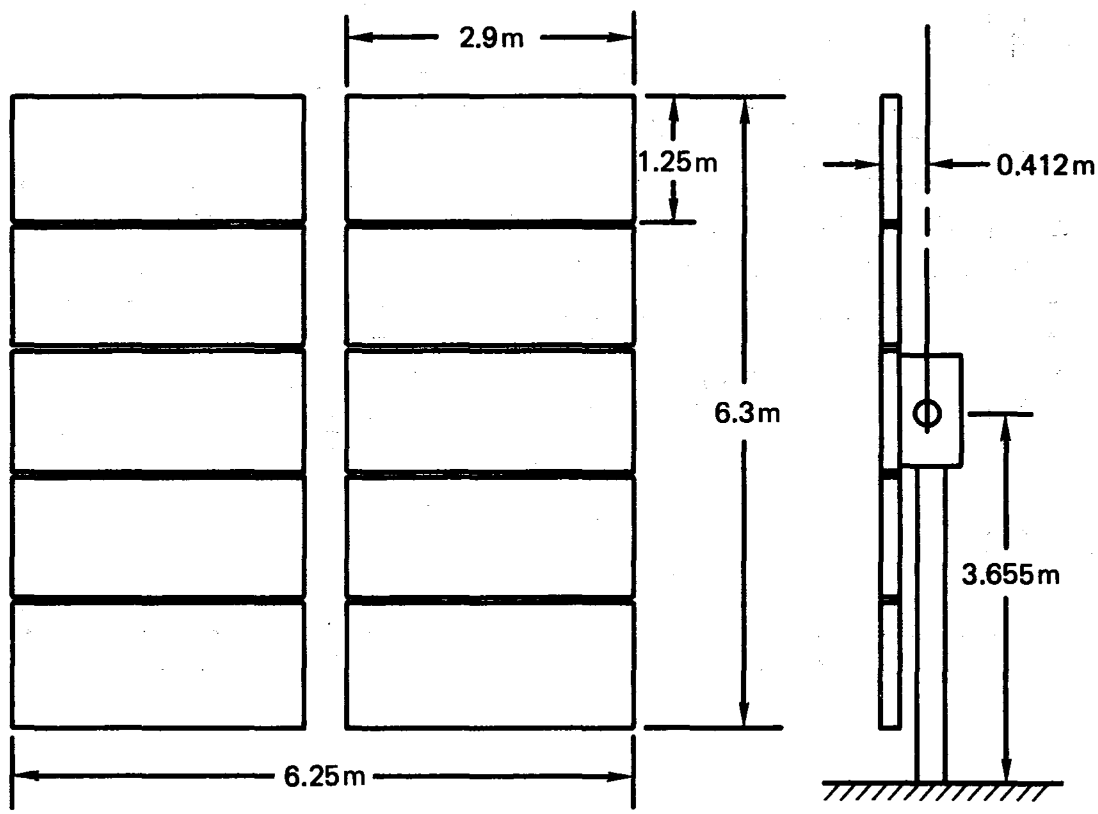

Figure 2. Heliostat Design

TABLE I

FACET FOCAL LENGTHS

Projection P(m)	0-69	69-122	122-170	170-205	205-232	232-∞
f(m)	85	118	160	202	226	255

The target (Figure 3) is a 3.4 m square centered at 0 m east, 5 m north, and 60 m above the center of the tower base. The target is inclined 21.8° downward. The tower shadow is modeled as that cast by a cylinder 71 m tall with radius of 5.5 m.

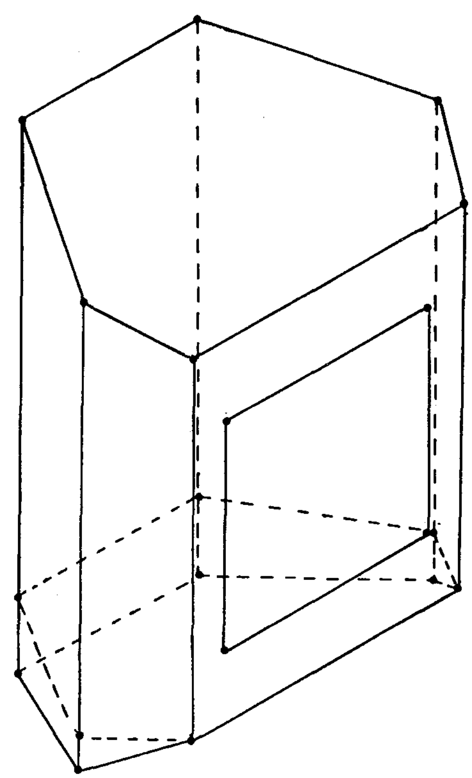

Figure 3. CESA-I Solar Receiver

The sun shape is taken as a uniform disk which subtends 9.29 mrad at the plant site. The calculation time is 10 A.M. on winter solstice. Insolation is 700 W/m^2. The latitude of the CESA-1 solar receiver site is 37.099°N. The atmospheric attenuation is modeled with Eq. (6.3-2) and (6.3-3) in Reference 2.

The dispersion in the error cone in HELIOS was set to 0.0033. In order to make the treatment of heliostat error sources consistent in the two codes, MIRVAL used 0.00165 rad for the standard deviation of the distribution function describing mirror-slope error and used no error in tracking angles. The users' guides[1-3] contain further description of the treatment of error sources.

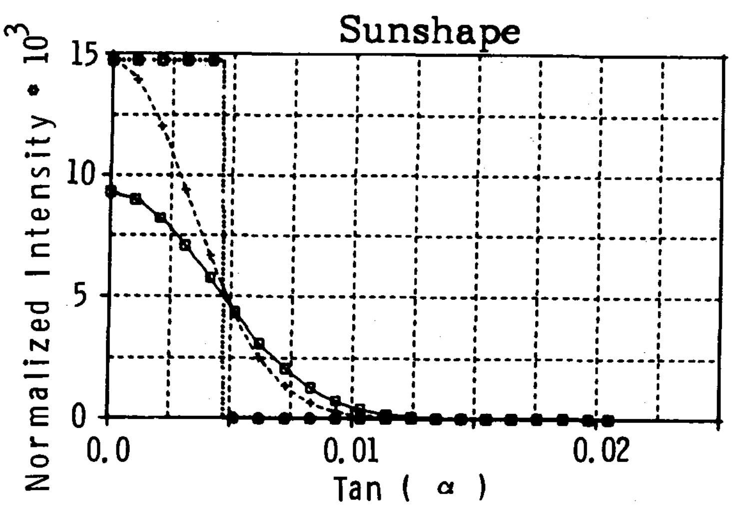

Figure 4. The uniform-disk sunshape (...), the error cone with a dispersion of 0.0033 (---), and the effective sunshape (——)

Result Comparisons

The field performance parameters calculated by HELIOS and MIRVAL for the power-tower system defined in the preceding section are listed below.

Power collected in aperture:		Error estimate
HELIOS	4.762 MW	0.013 MW (rough estimate - see section 7.1 of reference 2)
MIRVAL	4.786 MW	0.018 MW (the probability is 0.97 that the estimate differs from the true value by less than 0.018 MW)

Shadowing and blocking loss factor (area loss, not power loss at target):

HELIOS	0.92408	(.91888 for power loss at target)
MIRVAL	0.92541	(shadowing loss fraction 0.07149, blocking loss fraction 0.00334)

Cosine loss factor (caused by angle of incidence at facets):

HELIOS	0.94910
MIRVAL	0.94913

Spillage loss factor:

HELIOS	0.92174
MIRVAL	0.92142

Atmospheric attenuation loss factor:

HELIOS	0.97388
MIRVAL	0.97329

Flux density on target surface

This comparison is less straightforward since HELIOS calculates the flux density at a mesh of points while MIRVAL gives the average flux density in an array of bins. Integration over portions of the target mesh in HELIOS gives the power distribution on the target within a set of bins. By using the area of the bins the average flux density within each bin is calculated. This can then be compared with the MIRVAL output as shown in Table II. The target coordinates in the table have their origin at the target center with the x axis eastward and the y axis tilted from the vertical direction 21.8° toward the north. Horizontal slices of data near the peak are compared in Figure 5. Comparison of vertical slices of data near the peak gives similar agreement. Consistency in the results remains when all heliostat error sources are set to zero. Figures 6 and 7 are graphs of the flux density calculated by HELIOS.

TABLE II

FLUX DENSITY DISTRIBUTION ON APERTURE (MW/m^2)
FROM MIRVAL (HELIOS)

Target coordinates (in meters)

y \ x	1.70	1.02	0.34	-0.34	-1.02	-1.70
1.70						
	.0721 (.0746)	.1685 (.1702)	.2163 (.2353)	.1668 (.1732)	.0717 (.0761)	
1.02						
	.1918 (.1953)	.5852 (.5612)	.9176 (.9165)	.5795 (.5770)	.1998 (.2016)	
0.34						
	.2841 (.2770)	.9666 (.9124)	1.6760 (1.6302)	.9633 (.9386)	.2992 (.2872)	
-0.34						
	.1826 (.1901)	.5474 (.5469)	.8650 (.8862)	.5612 (.5564)	.1960 (.1955)	
-1.02						
	.0664 (.0712)	.1531 (.1639)	.2118 (.2247)	.1582 (.1641)	.0694 (.0724)	
-1.70						

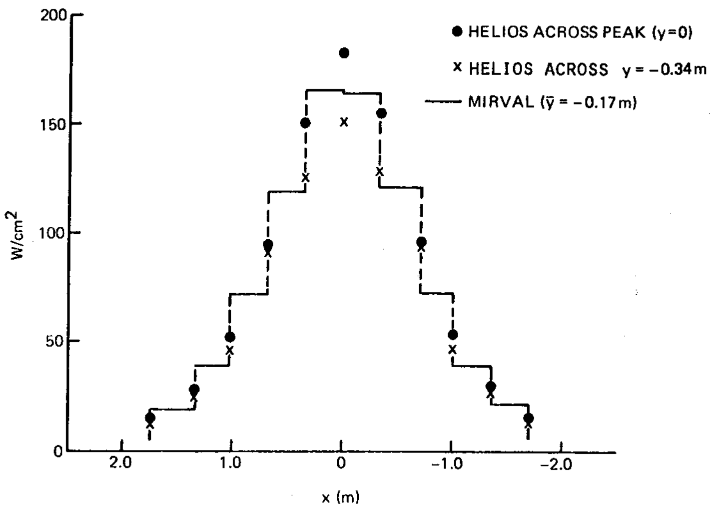

Figure 5. Horizontal Slices of Data Near Peak

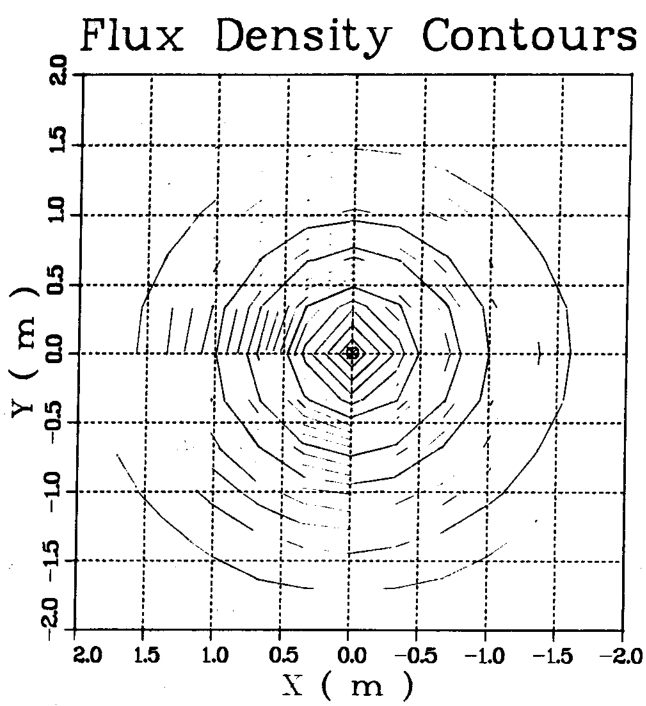

Figure 6. Isointensity contours of flux density on aperture at peak and (0.95 - 0.05I) for I = 0, 1, ..., 18. Greater density of data points is needed for good contour resolution near the peak

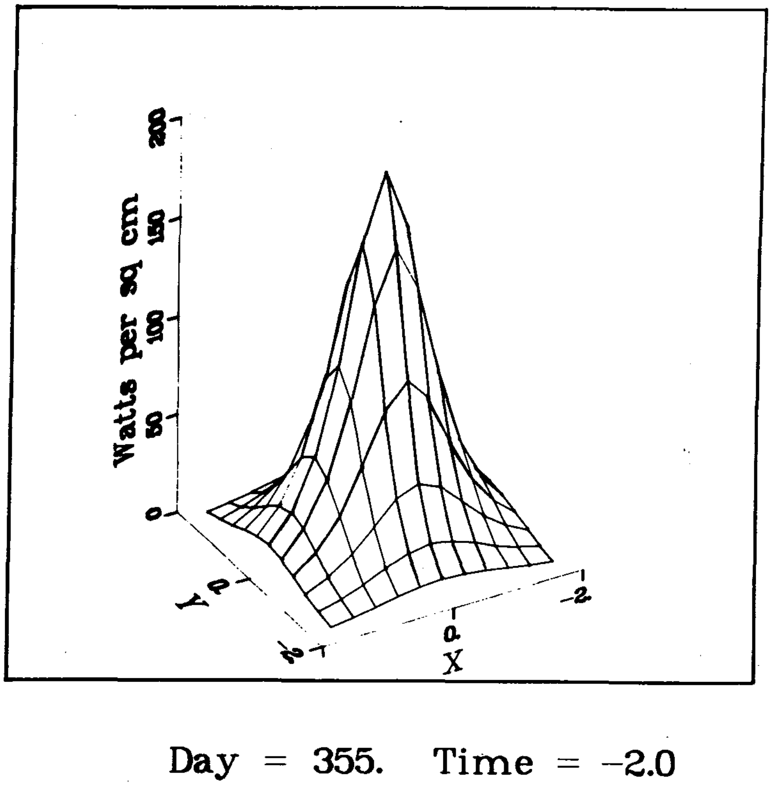

Figure 7. Flux Density Distribution on Aperture

More Detailed Shadowing and Blocking Comparison

The extent of shadowing and blocking in this calculation is illustrated in Figures 8-9. The blocking diagram is a projection of the outer edges of the heliostats onto a unit sphere centered at the target center. Overlap indicates that the closer heliostat blocks a portion of the light from the overlapped heliostat. The shadowing diagram is a projection of the outer edges of the heliostats and a projection of the receiver-tower model onto a plane orthogonal to the sun's rays. The cross-hatched section represents the tower. Overlap here indicates that the closer heliostat or the tower shadows a portion of a heliostat farther from the tower. Figures 8 and 9 show little blocking or shadowing other than the tower shadowing.

Early calculations indicated that the blocking results of MIRVAL and HELIOS were not consistent. A time shift to 4 P.M. (to emphasize the effect) and concentration upon heliostat number 136 (see Appendix) indicated this heliostat was being blocked by heliostat number 107. MIRVAL predicted the blocked fraction of the heliostat reflective area to be 0.0165. The corresponding HELIOS prediction was 0.042. Shortly before this discovery workers at INITEC[5] indicated an inconsistency between a HELIOS prediction for blocking and a hand calculation for this heliostat-field layout. Review of the code revealed the intent to locate the center of the unit sphere used for blocking at the center of the target. A programming error prevented these coordinates from being set, causing use of default CRTF parameters and thus the inconsistency. Code correction on July 5, 1979, made the MIRVAL, HELIOS and INITEC blocking results consistent. The shadowing and blocking diagrams for heliostats influencing number 136 at 4 P.M. are indicated in Figure 10.

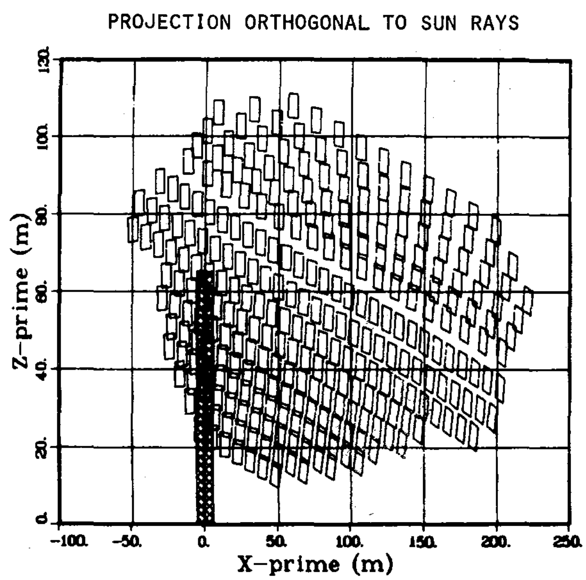

Figure 8. The Blocking Diagram

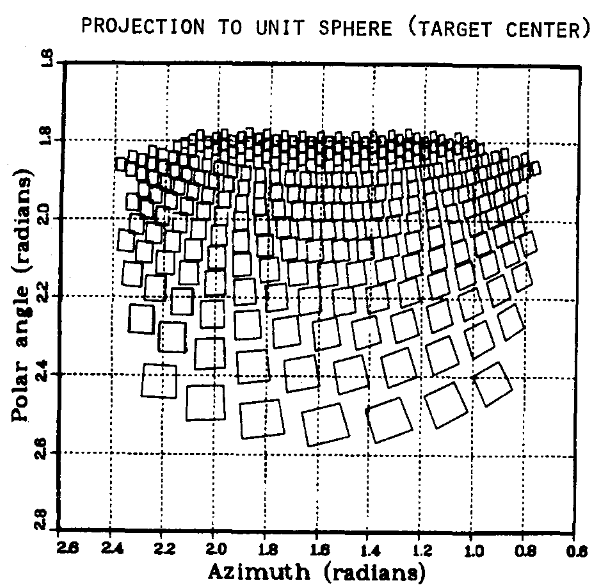

Figure 9. The Shadowing Diagram

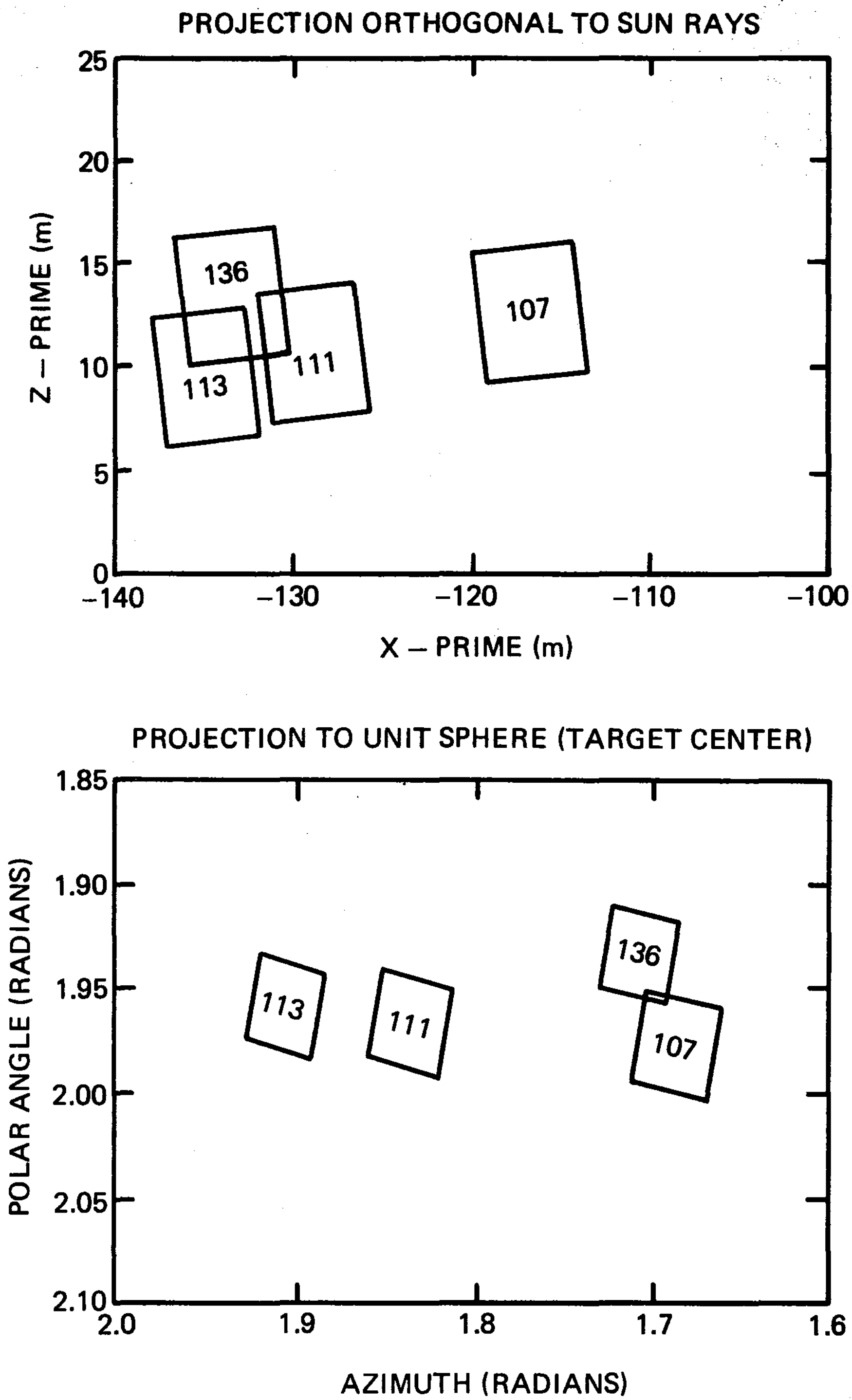

Figure 10. Shadowing and Blocking Diagrams Examining Heliostat Number 136 at 4 P.M. on Winter Solstice - The Top Graph Indicates Shadowing; The Bottom Blocking

Conclusions

With a uniform disk (pillbox) sunshape, and the preliminary power-tower design for the CESA-1 central receiver, the HELIOS-MIRVAL results are in good agreement. Descriptions of heliostat error sources can be selected in a consistent manner. No differences are apparent in predictions of the two computer codes. Since the codes are based upon widely different approaches (cone-optics vs Monte Carlo) this consistency indicates a measure of validity in the two approaches. Comparison with experimental data for a large field remains. Nevertheless, we have greater confidence in the codes because of this exercise.

APPENDIX--HELIOSTAT LAYOUT

COORDINATES OF HELIOSTAT MOUNTING STATIONS (IN METERS)
System origin is at the center of the tower base

Heliostat number	East	North	Vertical	Heliostat number	East	North	Vertical	Heliostat number	East	North	Vertical
1	0.00	45.00	0.00	96	60.00	120.00	0.00	191	-13.01	192.00	0.00
2	-10.00	45.00	0.00	97	-70.00	120.00	0.00	192	13.00	192.00	0.00
3	10.00	45.00	0.00	98	70.00	120.00	0.00	193	-26.08	192.00	0.00
4	-20.00	45.00	0.00	99	-80.00	120.00	0.00	194	26.08	192.00	0.00
5	20.00	45.00	0.00	100	80.00	120.00	0.00	195	-39.28	192.00	0.00
6	-30.00	45.00	0.00	101	-90.00	120.00	0.00	196	39.28	192.00	0.00
7	30.00	45.00	0.00	102	90.00	120.00	0.00	197	-52.67	192.00	0.00
8	-5.00	57.00	0.00	103	-100.00	120.00	0.00	198	52.67	192.00	0.00
9	5.00	57.00	0.00	104	100.00	135.00	0.00	199	-66.31	192.00	0.00
10	-15.00	57.00	0.00	105	-5.00	135.00	0.00	200	66.31	192.00	0.00
11	15.00	57.00	0.00	106	5.00	135.00	0.00	201	-80.27	192.00	0.00
12	-25.00	57.00	0.00	107	-15.00	135.00	0.00	202	80.27	192.00	0.00
13	25.00	57.00	0.00	108	15.00	135.00	0.00	203	-94.62	192.00	0.00
14	-35.00	57.00	0.00	109	-25.00	135.00	0.00	204	94.62	192.00	0.00
15	35.00	57.00	0.00	110	25.00	135.00	0.00	105	-109.42	192.00	0.00
16	-45.00	57.00	0.00	111	-35.00	135.00	0.00	206	109.42	192.00	0.00
17	45.00	57.00	0.00	112	35.00	135.00	0.00	207	-124.75	192.00	0.00
18	0.00	69.00	0.00	113	-45.00	135.00	0.00	208	124.75	192.00	0.00
19	-10.00	69.00	0.00	114	45.00	135.00	0.00	209	-6.91	204.00	0.00
20	10.00	69.00	0.00	115	-55.00	135.00	0.00	210	6.91	204.00	0.00
21	-20.00	69.00	0.00	116	55.00	135.00	0.00	211	-20.81	204.00	0.00
22	20.00	69.00	0.00	117	-65.00	135.00	0.00	212	20.81	204.00	0.00
23	-30.00	69.00	0.00	118	65.00	135.00	0.00	213	-34.77	204.00	0.00
24	30.00	69.00	0.00	119	-75.00	135.00	0.00	214	34.77	204.00	0.00
25	-40.00	69.00	0.00	120	75.00	135.00	0.00	215	-48.92	204.00	0.00
26	40.00	69.00	0.00	121	-85.00	135.00	0.00	216	48.92	204.00	0.00
27	-50.00	69.00	0.00	122	85.00	135.00	0.00	217	-63.32	204.00	0.00
28	50.00	69.00	0.00	123	-95.00	135.00	0.00	218	63.32	204.00	0.00
29	-60.00	69.00	0.00	124	95.00	135.00	0.00	219	-77.99	204.00	0.00
30	60.00	69.00	0.00	125	-105.00	135.00	0.00	220	77.99	204.00	0.00
31	-5.00	81.00	0.00	126	105.00	135.00	0.00	221	-93.05	204.00	0.00
32	5.00	81.00	0.00	127	-115.00	135.00	0.00	222	93.05	204.00	0.00
33	-15.00	81.00	0.00	128	115.00	135.00	0.00	223	-108.59	204.00	0.00
34	15.00	81.00	0.00	129	-125.00	135.00	0.00	224	108.59	204.00	0.00
35	-25.00	81.00	0.00	130	125.00	135.00	0.00	225	-124.59	204.00	0.00
36	25.00	81.00	0.00	131	-135.00	135.00	0.00	226	124.59	216.00	0.00
37	-35.00	81.00	0.00	132	135.00	135.00	0.00	227	0.00	216.00	0.00
38	35.00	81.00	0.00	133	0.00	152.00	0.00	228	-14.68	216.00	0.00
39	-45.00	81.00	0.00	134	-10.00	152.00	0.00	229	14.68	216.00	0.00
40	45.00	81.00	0.00	135	10.00	152.00	0.00	230	-29.43	216.00	0.00
41	-55.00	81.00	0.00	136	-20.00	152.00	0.00	231	29.43	216.00	0.00
42	55.00	81.00	0.00	137	20.00	152.00	0.00	232	-44.31	216.00	0.00
43	-65.00	81.00	0.00	138	-30.00	152.00	0.00	233	44.31	216.00	0.00
44	65.00	81.00	0.00	139	30.00	152.00	0.00	234	-59.43	216.00	0.00
45	-75.00	81.00	0.00	140	-40.00	152.00	0.00	235	59.43	216.00	0.00
46	75.00	81.00	0.00	141	40.00	152.00	0.00	236	-74.80	216.00	0.00
47	0.00	93.00	0.00	142	-50.00	152.00	0.00	237	74.80	216.00	0.00
48	-10.00	93.00	0.00	143	50.00	152.00	0.00	238	-90.57	216.00	0.00
49	10.00	93.00	0.00	144	-60.00	152.00	0.00	239	90.57	216.00	0.00
50	-20.00	93.00	0.00	145	60.00	152.00	0.00	240	-106.77	216.00	0.00
51	20.00	93.00	0.00	146	-70.00	152.00	0.00	241	106.77	216.00	0.00
52	-30.00	93.00	0.00	147	70.00	152.00	0.00	242	-123.45	216.00	0.00
53	30.00	93.00	0.00	148	-80.00	152.00	0.00	243	123.45	230.00	0.00
54	-40.00	93.00	0.00	149	80.00	152.00	0.00	244	-7.82	230.00	0.00
55	40.00	93.00	0.00	150	-90.00	152.00	0.00	245	7.82	230.00	0.00
56	-50.00	93.00	0.00	151	90.00	152.00	0.00	246	-23.53	230.00	0.00
57	50.00	93.00	0.00	152	-100.00	152.00	0.00	247	23.53	230.00	0.00
58	-60.00	93.00	0.00	153	100.00	152.00	0.00	248	-39.31	230.00	0.00
59	60.00	93.00	0.00	154	-110.00	152.00	0.00	249	39.31	230.00	0.00
60	-70.00	93.00	0.00	155	110.00	152.00	0.00	250	-55.31	230.00	0.00
61	70.00	93.00	0.00	156	-120.00	152.00	0.00	251	55.31	230.00	0.00
62	-80.00	93.00	0.00	157	120.00	152.00	0.00	252	-71.59	230.00	0.00
63	80.00	93.00	0.00	158	-130.00	152.00	0.00	253	71.59	230.00	0.00
64	-5.00	106.00	0.00	159	130.00	152.00	0.00	254	-88.18	230.00	0.00
65	5.00	106.00	0.00	160	-140.00	152.00	0.00	255	88.18	230.00	0.00
66	-15.00	106.00	0.00	161	140.00	152.00	0.00	256	-105.21	230.00	0.00
67	15.00	106.00	0.00	162	-5.00	171.00	0.00	257	105.21	230.00	0.00
68	-25.00	106.00	0.00	163	5.00	171.00	0.00	258	-122.78	230.00	0.00
69	25.00	106.00	0.00	164	-15.00	171.00	0.00	259	122.78	230.00	0.00
70	-35.00	106.00	0.00	165	15.00	171.00	0.00	260	0.00	244.00	0.00
71	35.00	106.00	0.00	166	-25.00	171.00	0.00	261	-16.63	244.00	0.00
72	-45.00	106.00	0.00	167	25.00	171.00	0.00	262	16.63	244.00	0.00
73	45.00	106.00	0.00	168	-35.00	171.00	0.00	263	-33.33	244.00	0.00
74	-55.00	106.00	0.00	169	35.00	171.00	0.00	264	33.33	244.00	0.00
75	55.00	106.00	0.00	170	-45.00	171.00	0.00	265	-50.19	244.00	0.00
76	-65.00	106.00	0.00	171	45.00	171.00	0.00	266	50.19	244.00	0.00
77	65.00	106.00	0.00	172	-55.00	171.00	0.00	267	-67.31	244.00	0.00
78	-75.00	106.00	0.00	173	55.00	171.00	0.00	268	67.31	244.00	0.00
79	75.00	106.00	0.00	174	-65.00	171.00	0.00	269	-84.73	244.00	0.00
80	-85.00	106.00	0.00	175	65.00	171.00	0.00	270	84.73	244.00	0.00
81	85.00	106.00	0.00	176	-75.00	171.00	0.00	271	-102.58	244.00	0.00
82	-95.00	106.00	0.00	177	75.00	171.00	0.00	272	102.58	244.00	0.00
83	95.00	106.00	0.00	178	-85.00	171.00	0.00	273	-8.83	259.00	0.00
84	0.00	120.00	0.00	179	85.00	171.00	0.00	274	8.83	259.00	0.00
85	-10.00	120.00	0.00	180	-95.00	171.00	0.00	275	-26.56	259.00	0.00
86	10.00	120.00	0.00	181	95.00	171.00	0.00	276	26.56	259.00	0.00
87	-20.00	120.00	0.00	182	-105.00	171.00	0.00	277	-44.38	259.00	0.00
88	20.00	120.00	0.00	183	105.00	171.00	0.00	278	44.38	259.00	0.00
89	-30.00	120.00	0.00	184	-115.00	171.00	0.00	279	-62.44	259.00	0.00
90	30.00	120.00	0.00	185	115.00	171.00	0.00	280	62.44	259.00	0.00
91	-40.00	120.00	0.00	186	-125.00	171.00	0.00	281	-80.82	259.00	0.00
92	40.00	120.00	0.00	187	125.00	171.00	0.00	282	80.82	259.00	0.00
93	-50.00	120.00	0.00	188	-135.00	171.00	0.00				
94	50.00	120.00	0.00	189	135.00	171.00	0.00				
95	-60.00	120.00	0.00	190	0.00	192.00	0.00				

REFERENCES

1. P. L. Leary and J. D. Hankins, A User's Guide for MIRVAL -- A Computer Code for Comparing Designs of Heliostat-Receiver Optics for Central Receiver Solar Power Plants, SAND77-8280, Sandia Laboratories, Livermore, California, February 1979.

2. F. Biggs and C. N. Vittitoe, The Helios Model for the Optical Behavior of Reflecting Solar Concentrators, SAND76-0347, Sandia Laboratories, Albuquerque, New Mexico, March 1979.

3. C. N. Vittitoe, F. Biggs, and R. E. Lighthill, HELIOS: A Computer Program for Modeling the Solar Thermal Test Facility, A Users Guide, SAND76-0346, Sandia Laboratories, Albuquerque, New Mexico, March 1977, Third Edition October 1978.

4. C. N. Vittitoe, F. Biggs, L. K. Matthews, and L. O. Seamons, Helios and Reconcentrators, Proceedings of the ISES Silver Jubilee 1979 International Congress, Atlanta, Georgia, May 28-June 1, 1979.

5. Private communication, F. Delgado of INITEC, June 28, 1979.

UNLIMITED RELEASE

INITIAL DISTRIBUTION

Elliott L. Katz, Director
Solar Thermal Projects
Energy Systems Group
The Aerospace Corporation
P.O. Box 92957
Los Angeles, CA 90009

G. W. Braun, Assistant Director
Solar Thermal Power Systems
Central Solar Energy Division
Department of Energy
Washington, DC 20545

G. M. Kaplan, Acting Chief
Large Solar Thermal Power Systems
Central Solar Energy Division
Department of Energy
Washington, DC 20545

H. H. Marvin, Deputy Program Director
Solar Geothermal and Electric Energy
Energy Technology Division
Department of Energy
Washington, DC 20545

C. J. Swet, Program Manager
Chemical and Thermal Storage Branch
Energy Storage Systems Division
Department of Energy
Washington, DC 20545

J. P. Zingeser
Large Power Systems Branch
Central Power Systems Division
Department of Energy
Washington, DC 20545

J. A. Blasy, Director
Solar Energy Division
Department of Energy
San Francisco Operations Office
1333 Broadway, Wells Fargo Building
Oakland, CA 94612

S. D. Elliott
Solar Energy Division
Department of Energy
San Francisco Operations Office
1333 Broadway, Wells Fargo Building
Oakland, CA 94612

R. W. Hughey, Deputy Division Director
Solar Energy Division
Department of Energy
San Francisco Operations Office
1333 Broadway, Wells Fargo Building
Oakland, CA 94612

R. N. Schweinberg
DOE STMPO
Suite 210
9650 Flair Park Drive
El Monte, CA 91731

John Bigger
Electric Power Research Institute
3412 Hillview Avenue
P.O. Box 10412
Palo Alto, CA 94304

Bill Masica
NASA-Lewis Research Center
21000 Brookpark Road
Cleveland, OH 44135

Jack Maddox
Public Service of New Mexico
P.O. Box 2267
Albuquerque, NM 87103

J. Lynn Rasband
Southern California Edison
P.O. Box 800
Rosemead, CA 91770

Ashok K. Seth
Solar Energy Group
Centre of Energy Studies
Indian Institute of Technology
Hauz Khas, New Delhi-110029, INDIA

McDonnell Douglas Astronautics Co.
Attn: R. H. McFee, J. B. Blackman,
J. R. Campbell
5310 Bolsa
Huntington Beach, CA 92647

D. Cahalan
Black & Veatch Consulting Engineers
P.O. Box 017F
11401 Lamar
Overland Park, KN 66211

Sanders Associates
Attn: S. B. Davis, N. McHugh
MER 12 1214
95 Canal Street
Nashua, NH 03060

Fernando Delgado
INITEC
Padilla 17
Madrid-6
SPAIN

Carlo Micheli
Snamprogetti
20097 S. Donato Milanese
Milano, ITALY

R. N. Singh
Dept. of Physics
Indian Institute of Technology
New Delhi-29, INDIA

A. Divecchia
C.T.I.P. International
30 Rockefeller Plaza
New York, NY 10020

Gershon Grossman
Israel Institute of Technology
Faculty of Mechanical Engineering
Technion City, Haifa 32000
ISRAEL

G. D. Gupta
Foster Wheeler Development Corp.
12 Peach Tree Hill Road
Livingston, NJ 07039

Solar Energy Research Institute
Resource Assessment Branch
Attn: R. Hulstrom, J. Williamson,
B. Butler, K. Touryan
1536 Cole Boulevard
Golden, CO 80401

General Electric
Attn: R. H. Horton, W. F. Knightly
1 River Road, Building 23, Room 334
Schenectady, NY 12345

Stuart Schwartz
General Electric
1 River Road, Building 6, Room 329
Schenectady, NY 12345

C. Thomas Brown
Solar Energy & Materials Technology Div.
Engineering Experiment Station
Georgia Institute of Technology
Atlanta, GA 30322

Black & Veatch
Attn: M. Wolf, S. L. Levy,
J. T. Davis
P.O. Box 8405
Kansas City, MO 64114

University of Houston
Solar Energy Laboratory
Attn: Fred Lipps,
L. Vant-Hull
4800 Calhoun
Houston, TX 77004

Acurex Corporation
Alternate Energy Division
Aerotherm Group
Attn: Peter Overly, Donald Brink
485 Clyde Avenue
Mountain View, CA 94042

Tony Curinga
General Electric ESPD
Building 6, Room 329
Schenectady, NY 12345

Westinghouse Advanced Energy
Systems Division
Attn: J. Day, D. Hofer, M. Lipner
W. Parker, W. Pierce, C. Silverstein
P.O. Box 10864
Pittsburgh, PA 15236

A. J. Poche
General Electric Company
Space Division
Room 7246 CC&F #7
P.O. Box 8555
Philadelphia, PA 19101

Jet Propulsion Laboratory
Attn: P. Poon, MS 506-328
V. Truscello, MS 502-201
4800 Oak Grove Drive
Pasadena, CA 91103

Martin Marietta
Attn: W. Hart, MS S0510
G. A. Roe, MS S0510
P. Norris, MS S0403
J. Montague, MS S0403
T. Oliver, MS S0403
P.O. Box 179
Denver, CO 80201

D. Wolfe
Dynatherm Corporation
One Industry Lane
Cockeysville, MD 21030

G. Yenatchi
Gruman Energy Systems
4175 Veterans Memorial Highway
Ronkonkona, NY 11779

R. L. Lessley, 301-3
Bechtel Corporation
P.O. Box 3965
San Francisco, CA 94119

F. A. Blake
7102 South Franklin Street
Littleton, CO 80122

E. J. Valley
Boeing Engineering and Construction
P.O. Box 3707
Seattle, WA 98124

C. G. Howard
Booz, Allen & Hamilton, Inc.
8801 E. Pleasant Valley Road
Cleveland, OH 44131

G. P. Mulholland
New Mexico State University
Dept. of Mechanical Engineering
P.O. Box 3450
Las Cruces, NM 81803

D. R. McCullough
Acurex Corporation
485 Clyde Avenue
Mountain View, CA 94042

J. L. Mortley, 1521
N. R. Keltner, 1537
F. W. Neilson, 1550
E. A. Igel, 1556
B. J. Tolman, 3151
G. Yonas, 4200
J. B. Gerardo, 4210
J. E. Powell, 4230
J. H. Renken, 4231
F. Biggs, 4231
R. E. Lighthill, 4231
C. N. Vittitoe, 4231 (15)
G. W. Kuswa, 4240
T. H. Martin, 4250
J. H. Scott, 4700
G. E. Brandvold, 4710
B. W. Marshall, 4713
D. B. Davis, 4713
J. T. Holmes, 4713
D. L. King, 4713
L. K. Matthews, 4713
L. O. Seamons, 4713
B. D. Shafer, 4719
V. L. Dugan, 4720
J. V. Otts, 4721
J. F. Banas, 4722
R. W. Harrigan, 4722
G. W. Treadwell, 4722
T. A. Dellin, 4723
R. R. Peters, 4723
J. A. Leonard, 4725
E. L. Harley, 4725
J. C. Zimmerman, 4725
R. J. Gross, 5512
J. R. Koteras, 5523
T. B. Cook, 8000, Attn: W. J. Spencer, 8100
A. N. Blackwell, 8200
L. Gutierrez, 8400
B. F. Murphey, 8300; Attn: D. M. Schuster, 8310
R. L. Rinne, 8320
W. Bauer, 8340
D. L. Hartley, 8350
M. J. Fish, 8326
J. D. Hankins, 8326
G. W. Anderson, 8330
R. J. Kee, 8331
P. L. Leary, 8331 (25)
R. E. Huddleston, 8332
A. G. Schuknecht, 8333
R. Y. Lee, 8334
C. S. Selvage, 8420
R. C. Wayne, 8450
A. F. Baker, 8450
P. J. Eicker, 8451

T. D. Brumleve, 8451
C. J. Pignolet, 8451
A. C. Skinrood, 8452
W. G. Wilson, 8453

P. Dean, 8265/Technical Library Processes Division, 3141
Technical Library Processes Division, 3141 (5)
W. L. Garner, 3151 (3)
R. P. Campbell for DOE/TIC (27), 3154
Library and Security Classification Division, 8266-2 (3)